

Multi-anode photomultiplier tube as a tool for spatio-temporal measurements in a plasma

Ole Waldmann and Werner Bohmeyer

Max-Planck-Institut fuer Plasmaphysik, EURATOM Association, Wendelsteinstr. 1, D-17491 Greifswald, Germany

Measurements of fast phenomena in the vicinity of a limiter inserted into a linear plasma column are shown in this work. The results were conducted at the plasma generator PSI-2 (Humboldt Universitaet zu Berlin, Germany) which provides a stationary plasma produced in a DC arc discharge. The plasma near a tungsten limiter was imaged on a photomultiplier tube equipped with 16 anodes. The photomultiplier array was being attached to oscilloscopes. In comparison with fast cameras this arrangement is inferior with respect to spatial resolution but superior with regard to temporal resolution which is more important in the present context. Two different structures with enhanced photon emission regions were investigated. On the one hand the rotation of the plasma column could be seen, with and without limiter. On the other hand, when immersing limiters inside the column structures with a high photon emission travelling radially into the shadow downwards the limiter were investigated. These investigations deal with basic questions, they could help to understand the anomalous transport in linear devices in general and the transport in plasma shadows behind limiters in particular.

Keywords: convective plasma transport, plasma blobs, optical diagnostics, plasma rotation

1. Introduction

Observing the plasma in the vicinity of a material limiter on a short time scale can provide information about intermittent processes possibly being responsible for an anomalous transport. In an earlier paper anomalous transport was proposed for the linear plasma generator PSI-2 [1] but a convincing explanation how this transport mechanism works could not be given.

The enhanced transport perpendicular to the magnetic field lines in magnetically confined plasma was explained by Antar et al. [2] with a convective transport process. This anomalous transport cannot only be found in toroidal but also in linear configurations [3]. In the just mentioned works Langmuir probes and fast imaging cameras were used as diagnostics.

Groups at other linear devices investigated intermittent transport processes in the past [4–7], other references can be found in the review article about turbulence in toroidal devices by Zweben et al. [8]. In the frame of this work Carter's article [6] is especially interesting, because limiters were also used in that work. But the plasma was a non-stationary and non-rotating one (pulses of 10 ms), compare section 2.1 for the plasma used in this work. He measured a fairly high amount of density in the shadow of the limiter as it was also shown by us in the past [9]. He used arrays of negatively biased Langmuir probes which measured enhanced signals moving outwards and decreased signals moving inwards stochastically with a velocity of at least $1000 \frac{\text{m}}{\text{s}}$. Our probe measurements in the past were not in an array but in a single probe configuration and too slow to measure such intermittent events.

One advantage of an optical measurement is its non-invasive nature. The mentioned fast cameras can be used

with short exposure times ($t \approx 1 \mu\text{s}$) but have long read out times between frames ($t = 10 \mu\text{s}$). It is shown in the following that such long intermissions in between frames would not be tolerable.

The measurements presented in this work were performed using a multi-anode photomultiplier, which will be described in section 2.2. This diagnostic tool has already been used in other field of physics [10–12], but not in plasma diagnostics. For the observation of the scrape-off layer in NSTX two rectangularly crossed lines of photomultipliers were used [13], which cannot provide a full two-dimensional spatial resolution. In the course of this work, we will first introduce the plasma generator PSI-2, the multi-anode photomultiplier and the limiters briefly. In the main part of this work we will concentrate on the measurements with and without limiter and afterwards conclude the article.

2. Experimental Setup

2.1 Plasma Generator PSI-2

PSI-2 is a linear plasma device with a stationary arc discharge. A steady discharge current in the range of 20 to about 500 A can be chosen. The plasma is produced in the discharge region which consists of a heated, hollow, cylindrical LaB₆-cathode and a cylindrically-shaped Mo-anode. This leads to a hollow profile in electron density and temperature. Guided by an axial magnetic field the plasma streams with a typical cross-section of 60 mm through a so called differential pumping system and a target chamber until it is terminated at a neutralizer plate (cf. Fig. 1). The limiter was placed in the first target plane and the optical system was installed under a rectangular angle to the plasma (cf. Fig. 1). We used helium and argon as working gases. Typical plasma parameters are: $I_{\text{AC}} = 50 \dots 200 \text{ A}$,

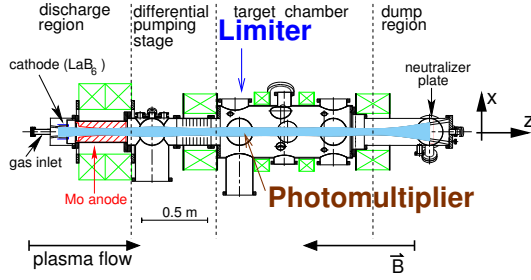


Fig. 1 Plasma Generator PSI-2.

$$B = 0.1 \text{ T}, n_e = 1 \dots 5 \cdot 10^{18} \text{ m}^{-3}, T_e = 2 \dots 15 \text{ eV}, \\ T_i = 0.5 \dots 0.7 T_e, p_{\text{neutral}} \approx 0.05 \text{ Pa}.$$

2.2 Multi-Anode Photomultiplier

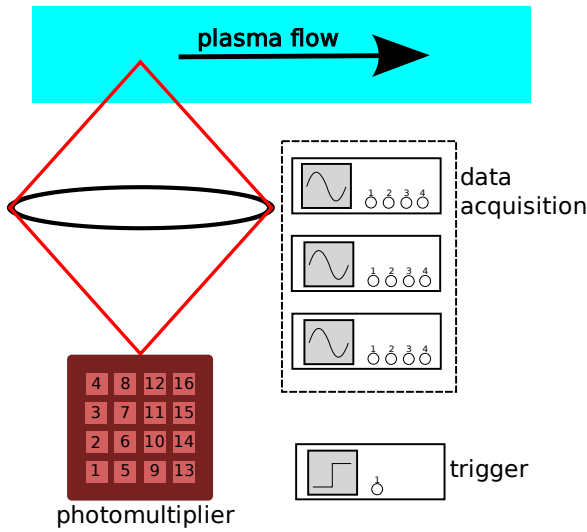


Fig. 2 Multi-anode photomultiplier with four oscilloscopes. Three for data acquisition and one for their external triggering.

To achieve a high temporal resolution, a photomultiplier (*PMT*) was used in this work. To obtain also spatial resolution we used a multi-anode photomultiplier (Hamamatsu H6568-01) [14]. It consists of a photo cathode, an arrangement of dynodes and sixteen anodes. The setup strives for compactness to minimize the influence of an external magnetic field.

A 4×4 -grid is installed in front of the photo cathode and with the arrangement of the dynodes each cell of this grid is mapped to one anode. The cross-talk between neighbored channels is very small ($< 1\%$ [11]). Each channel is calibrated and normalized on its own to handle with the unequal sensitivity of the channels.

A lens maps the plasma onto the photomultiplier. A grey filter and a narrow band interference filter (589 nm in the case of helium and 435 nm in the case of argon) were set in between the lens and the photomultiplier. For the data acquisition three fast oscilloscopes with four channels each (Tektronix TDS 540A, 744A, 754C) were used. A fourth

oscilloscope (Tektronix 2440) was used to trigger the other three oscilloscopes simultaneously (cf. Fig. 2). One channel of the photomultiplier was used as a trigger signal. All oscilloscopes measure continuously. Therefore, pre-trigger events were also measured. The three oscilloscopes were connected to a computer via GPIB and controlled by this computer.

The background signal was quite high therefore all channels were attached to the oscilloscopes in AC. This improved the signal-to-noise ratio for the interesting fluctuations. When measuring in AC configuration (cf. Fig. 3) one has to consider the critical frequency $f_{\text{crit}} = \frac{1}{2\pi C_c R_t}$ with C_c as the coupling capacitor and R_t as the terminating resistor [15]. The frequency of the signals in our case was much higher than the critical frequency $f_{\text{crit}} \approx 10 \text{ Hz}$ ($C_c = 0.016 \mu\text{F}$, $R_t = 1 \text{ M}\Omega$).

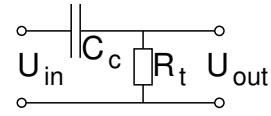


Fig. 3 Capacitor coupling with the coupling capacitor C_c , the terminating resistor R_t , input U_{in} , and output voltage U_{out} , respectively.

2.3 Limiters

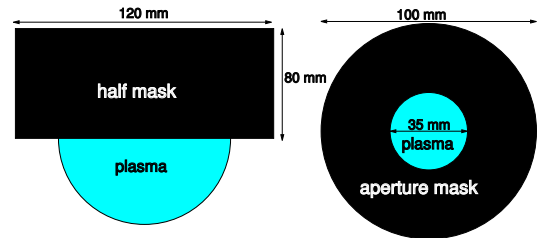


Fig. 4 Limiters used in the investigations.

Two kinds of limiters were used. Both are made of tungsten and brought into the plasma under floating conditions. First is a rectangular mask which cuts away half the plasma (*half mask* (HM)), the second one has an orifice with an opening of 35 mm (*aperture mask* (AM)). The half mask breaks the rotational symmetry of the plasma while the aperture mask cuts away the hotter and denser part of the plasma column.

3. Experimental Results

3.1 Movement Without Limiter

For the collective movement we set up a trigger threshold to measure enhanced or reduced intensity. The trigger was set to significant events. We averaged the signals over 50 events.

In Fig. 5 twelve channels are shown at different times. The successive response of the different lines is very obvious. First, the line at $x \approx -3 \text{ mm}$ gains intensity, afterwards

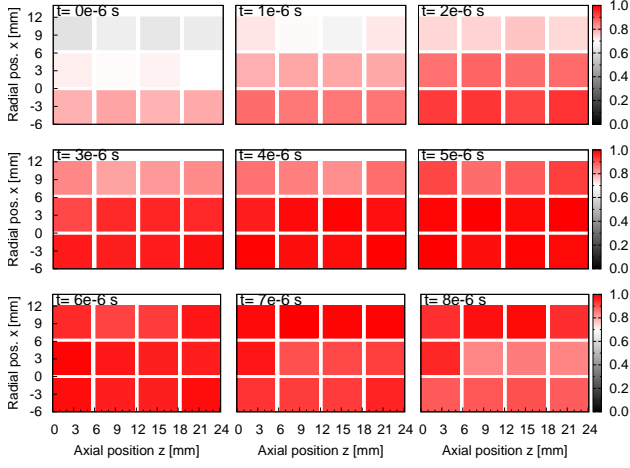


Fig. 5 Argon discharge without limiter. Rotational movement of enhanced intensity. Averaged measurement.

the line at $x \approx 3$ mm and at last the line at $x \approx 9$ mm. The reduction of the signal happens in the same manner. This looks like a rotation of the plasma column with a non-homogeneous intensity distribution in the column. Klose [16] showed in his PhD thesis a rotating five-fold structure in a krypton plasma, with enhanced intensity in the corners at a radius $r_m = 27.6$ mm. The rotational frequency was determined to $f_{\text{rot}} = 12$ kHz.

In our case we have an average distance of 6 mm between the channels and the structure moves with $1.2 \mu\text{s}$ from channel to channel. Assuming the same radius as in krypton, this results in a velocity and frequency of

$$v \approx \frac{6 \text{ mm}}{1.2 \mu\text{s}} = 5000 \frac{\text{m}}{\text{s}}, \quad (1)$$

$$f_{\text{rot}} = \frac{v}{2\pi r} = 29 \text{ kHz}. \quad (2)$$

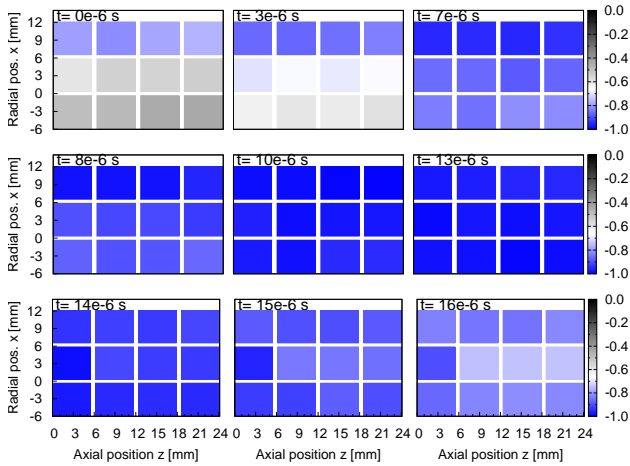


Fig. 6 Argon discharge without limiter. Rotational movement of reduced intensity. Averaged measurement.

Taking the $1/m_i$ -dependency of rotational frequency,

where m_i is the ion mass, into account and supposing the same five-fold structure, this is roughly comparable to the rotation in krypton. We found $(f_{\text{rot}} \cdot m_i)|_{\text{Ar}} / (f_{\text{rot}} \cdot m_i)|_{\text{Kr}} = 1.15$ as the ratio of the products of rotational frequency and ion mass. The sequence of the successive response of lines corresponds with the sense of rotation of the plasma column measured by spectroscopy. This supports the assumption of an observation of a rotation of the plasma column while looking at the collective movement. It should be emphasized that the temporal resolution is very important for the observation of this movement. A fast camera with a read out time of about $10 \mu\text{s}$ would not be able to reveal the whole process.

Looking closer at the reduced intensity (Fig. 6) the line by line behaviour can be recovered but in the inverted direction. However, due to the much broader signal an estimation of the velocity would be less accurate.

3.2 Movement with Limiters

The measurement shown in Fig. 7 is again an average like in the case without limiter. But this time the half mask is inserted at $z = 0$ mm and blocks the positive x -half space (the mask is marked in green in the figure). By comparison with Fig. 5 the same rotational movement with a similar velocity can be found. The only difference is the behavior of plasma in the column directly behind the mask. The movement in this column at $z \approx 3$ mm is delayed in comparison with the columns at bigger z -values.

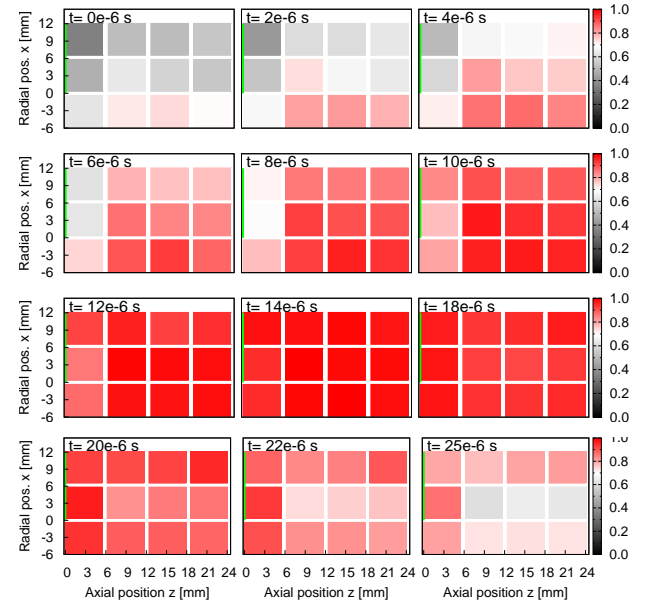


Fig. 7 Argon discharge with half mask (positive x -half space at $z = 0$ mm, marked in green). Averaged measurement.

Besides this collective movement which can be found with and without a limiter, quite a different structural behaviour also shows up in the case with limiter. Because of the stochastic appearance of these events we refer to non-averaged measurements in the following.

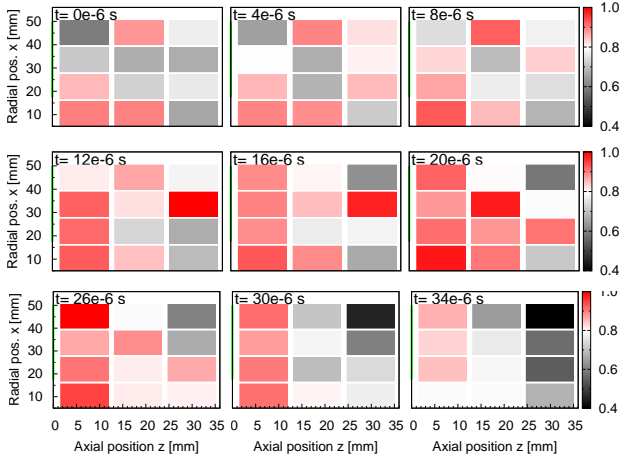


Fig. 8 Helium discharge with aperture mask ($x \geq 17.5$ mm at $z = 0$ mm, marked in green). Single measurement.

First a measurement in helium with the aperture mask is shown in Fig. 8. The orifice has a radius of 17.5 mm and its center is positioned at plasma axis $x = 0$ mm, $z = 0$ mm. The signal in this single measurement is quite noisy but one can see that there is an enhanced intensity pattern moving radially outwards directly behind the aperture mask. This movement differs from the collective one in a way that not a whole line gains intensity at the same time. The pattern is mostly in the first column after the limiter with a slight overlap to the second column. The radial movement will be more noticeable in the next example.

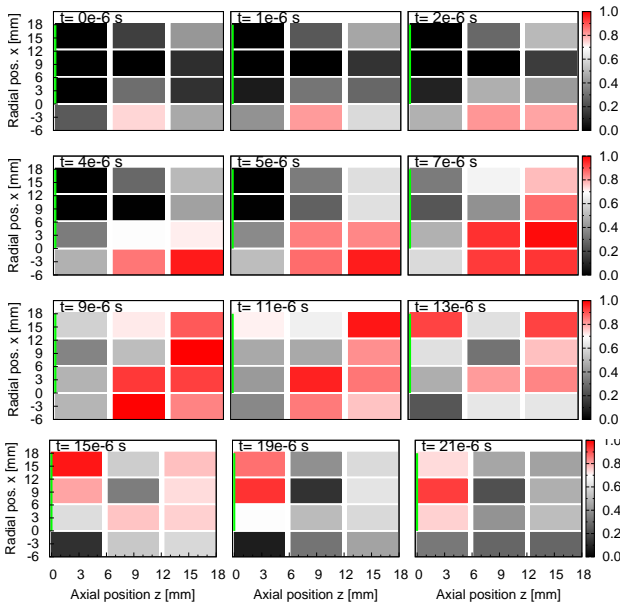


Fig. 9 Argon discharge with half mask (positive x -half space at $z = 0$ mm, marked in green). Single measurement.

In the measurement shown in Fig. 9 the half mask is set to the positive x -half space at $z = 0$ mm. At the time step $t = 0 \mu\text{s}$ one cell inside the plasma column shows an enhanced intensity. This cell is moving into the shadow of

the limiter and decreases after $15 \mu\text{s}$. Afterwards it shows up again directly behind the limiter moving towards the undisturbed plasma. This can be interpreted as a convective transport in a spiral movement.

These single measurements showed small spatial structures which moves independently from the rest of the plasma into the shadow of the limiter. In both cases with masks we can measure radial velocities of about $3000 \frac{\text{m}}{\text{s}}$. As a comparison the streaming velocity of undisturbed plasma in PSI-2 should be mentioned which is in the range of $500 \frac{\text{m}}{\text{s}}$ [17].

3.3 Temporal Behaviour

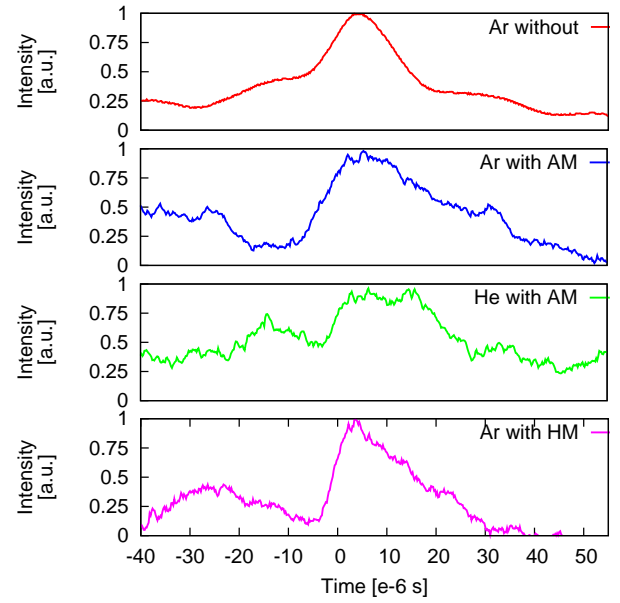


Fig. 10 Time traces of intensity in one cell. First measurement is averaged over 50 times. The other three measurement are single measurements.

Looking at the temporal behaviour of the events a classification can be made by the ratio of the rise time to the decay time, cf. Fig. 10. In this figure the intensity of a particular cell is depicted. Especially the event with the half mask shows a very fast rise and a slow decay. The different events are summarized in Table 1 and compared to a value of a blobby event in PISCES measured with Langmuir probes [3].

Experiment	Ar _{without}	Ar _{AM}	He _{AM}	Ar _{HM}	[3]
$t_{\text{incr}}/t_{\text{decr}}$	0.9	0.4	0.3	0.2	0.2

Table 1 Ratio of rise time to decay time (cf. Fig. 10).

There are other groups (e.g. [18–20]) which observed intermittent structures that can be assigned to convective transport. In the case of an optical measurement one has to recall that electron temperature has a much stronger effect on

visibility than electron density. But the combined measurements of Langmuir probes and fast cameras undertaken by the just mentioned groups suggest that these enhanced intensity events are due to density perturbations and therefore blobby plasma transport.

4. Conclusion

In this work we showed the use of a multi-anode photomultiplier as a tool to measure fast phenomena with moderate spatial resolution.

The advantage of this method in comparison to fast cameras is the possibility of taking data continuously without intermission for read out. This gave us the opportunity to see intermittent events on a very short time scale.

We could distinguish between two movements. A collective one which could be interpreted as a rotation of the whole plasma column, and a convective one, indicating transport of small structures into the shadow of a limiter.

The movement of enhanced intensity cells into the shadow of a limiter across magnetic field lines could be a possible explanation for the unexpected high density level in these shadows. To decide if these events contribute to particle and/or heat transport it is intended to combine these optical measurements with probe arrays in the future.

- [1] O. Waldmann et al., Contributions to Plasma Physics **47**, 692 (2007).
- [2] G.Y. Antar et al., Physical Review Letters **87**, 6 (2001).
- [3] G.Y. Antar et al., Physics of Plasmas **10**, 419 (2003)
- [4] A.H. Nielsen et al., Physics of Plasmas **3**, 1530 (1996)
- [5] G. Y. Antar et al., Physics of Plasmas **14**, 022301 (2006).
- [6] T.A. Carter, Physics of Plasmas **13**, 010701 (2006)
- [7] T. Windisch et al., Physics of Plasmas **13**, 122303 (2006)
- [8] S.J. Zweben et al., Plasma Physics and Controlled Fusion **49**, S1 (2007)
- [9] O. Waldmann et al., AIP Conference Proceedings **812**, 443 (2006)
- [10] A.J. Soares et al., Nuclear Instruments and Methods in Physics Research Section A **477**, 77 (2002)
- [11] P. Krizan et al., Nuclear Instruments and Methods in Physics Research Section A **394**, 27 (1997)
- [12] E. Albrecht et al., Nuclear Instruments and Methods in Physics Research Section A **488**, 110 (2002)
- [13] M. Agostini et al., Physics of Plasmas **14**, 102305 (2007)
- [14] H. Kyushima et al., IEEE Transactions on Nuclear Science **41**, 725 (1994).
- [15] G. Meyer, *Oszilloskope* (Huethig, Heidelberg, 1989)
- [16] S. Klose, PhD thesis, Humboldt Universitaet zu Berlin, Germany (2000)
- [17] T. Lunt et al., Physical Review Letters **100**, 175004 (2008)
- [18] N. Ohno et al., Journal of Plasma and Fusion Research **80**, 275 (2004)
- [19] S.H. Müller et al., Physics of Plasmas **13**, 100701 (2006)
- [20] C. Theiler et al., Physics Plasmas **15**, 042303 (2008)